CHAPTER 6

INCREASE IN SHORT-CHAIN CERAMIDES CORRELATES WITH AN ALTERED LIPID ORGANIZATION AND DECREASED BARRIER FUNCTION IN ATOPIC ECZEMA PATIENTS

Jeroen van Smeden[1,*], Michelle Janssens[1,*], Gert S. Gooris[1], Wim Bras[2], Guiseppe Portale[2], Peter J. Caspers[3,4], Rob J. Vreeken[5,6], Thomas Hankemeier[5,6], Sanja Kezic[7], Ron Wolterbeek[8], Adriana P.M. Lavrijsen[9], and Joke A. Bouwstra[1]

[1] Division of Drug Delivery Technology, Leiden Academic Centre for Drug Research, Leiden University, Leiden, The Netherlands.
[2] Netherlands Organization for Scientific Research, DUBBLE CRG/ESRF, Grenoble, France.
[3] Center for Optical Diagnostics and Therapy, Department of Dermatology, Erasmus MC, Rotterdam, The Netherlands.
[4] River Diagnostics BV, Rotterdam, The Netherlands.
[5] Division of Analytical Biosciences, Leiden Academic Centre for Drug Research, Leiden University, Leiden, The Netherlands.
[6] Netherlands Metabolomics Centre, Leiden Academic Centre for Drug Research, Leiden University, Leiden, The Netherlands.
[7] Coronel Institute of Occupational Health, Academic Medical Center, University of Amsterdam, Amsterdam, The Netherlands.
[8] Department of Medical Statistics and Bioinformatics, Leiden University Medical Center, Leiden, The Netherlands.
[9] Department of Dermatology, Leiden University Medical Center, Leiden, The Netherlands.
*Both authors contributed equally to this work

Adapted from Journal of Lipid Research. 2012. 53:2755-2766.

Abstract

A hallmark of atopic eczema (AE) is skin barrier dysfunction. Lipids in the stratum corneum (SC), primarily ceramides, free fatty acids and cholesterol, are crucial for the barrier function, but their role in relation to AE is indistinct. Filaggrin is an epithelial barrier protein with a central role in the pathogenesis of AE. Nevertheless, the precise causes of AE-associated barrier dysfunction are largely unknown. In this study, a comprehensive analysis of ceramide composition and lipid organization in non-lesional SC of AE patients and control subjects was performed by means of mass spectrometry, infrared spectroscopy, and X-ray diffraction. In addition, the skin barrier and clinical state of the disease were examined. The level of ceramides with an extreme short chain length is drastically increased in SC of AE patients, which leads to an aberrant lipid organization and a decreased skin barrier function. Changes in SC lipid properties correlate with disease severity but are independent of filaggrin mutations. We demonstrate for the first time that changes in ceramide chain length and lipid organization are directly correlated with the skin barrier defects in non-lesional skin of AE patients. We envisage that these insights will provide a new therapeutic entry in therapy and prevention of AE.

Introduction

The skin offers a protective barrier against allergens, irritants, and microorganisms and prevents excessive transepidermal water loss (TEWL). The barrier function strongly relies on the outermost layer of the skin, the stratum corneum (SC), which consists of corneocytes embedded in a highly organized lipid matrix[1,2]. This lipid matrix is

considered to be important for a proper skin barrier function.

Ceramides (CERs), cholesterol, and free fatty acids are the main lipid classes in SC. To date, 12 CER subclasses in human SC have been identified with a wide chain length distribution[3,4]. An explanation of the CER nomenclature is given in Figure 1. The aim of the present study was to determine the chain lengths of each CER subclass in non-lesional skin of atopic eczema (AE) patients and to correlate these with lipid organization, skin barrier function and disease severity, see Figure 2.

AE is a chronic relapsing inflammatory skin disease characterized by a broad spectrum of clinical manifestations, such as erythema, dryness, and intense pruritus[5,6]. AE affects over 15% of Caucasian children and 2-10% of adults, and its prevalence is increasing rapidly, especially in developed countries[7-11]. Patients have a decreased skin barrier

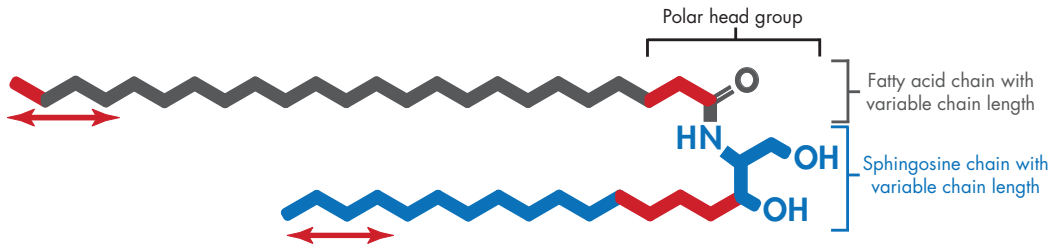

	Non-hydroxy fatty acid [N]	α-hydroxy fatty acid [A]	Esterified ω-hydroxy fatty acid [EO]
Dihydrosphingosine [dS]	[NdS]	[AdS]	[EOdS]
Sphingosine [S]	[NS]	[AS]	[EOS]
Phytosphingosine [P]	[NP]	[AP]	[EOP]
6-hydroxy sphingosine [H]	[NH]	[AH]	[EOH]

Figure 1: *Structure and nomenclature of CERs. All CERs bear a polar head group and two long carbon chains. The polar head group may vary in molecular architecture (at the carbon positions marked in red), resulting in 12 different subclasses in human SC. Both chains in every CER subclass show varying carbon chain lengths (marked by red arrows). Each CER subclass is denoted by its sphingoid base (blue) and fatty acid chain (gray), resulting in the 12 CER subclasses. The abbreviations are as follows: For the sphingoid base: dihydrosphingosine (dS), sphingosine (S), phytosphingosine (P), 6-hydroxy sphingosine (H). The various acyl chains are denoted by: Non-hydroxy fatty acid (N), α-hydroxy fatty acid (A) and esterified ω-hydroxy fatty acid (EO). This results in the 12 CER subclass notations: [NdS], [AdS], [EOdS], [NS], [AS], [EOS], [NP], [AP], [EOP], [NH], [AH], [EOH]. The number of total carbon atoms in the CERs (e.g. C34 CERs) is the number of carbon atoms in the fatty acid chain plus the number of carbon atoms in the sphingoid base.*

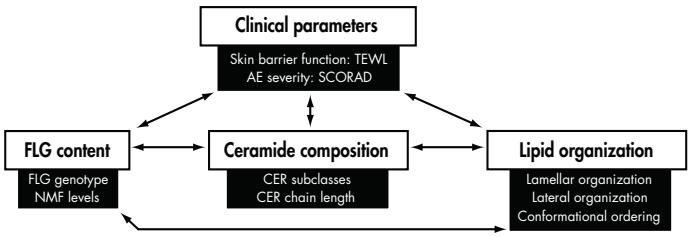

Figure 2: *Schematic overview of the SC lipid parameters, clinical parameters, and the determinants of the filaggrin content discussed in this article. These different parameters may all affect the skin barrier and are therefore investigated in this study. Arrows indicate possible correlations that are studied throughout the manuscript.*

function in lesional and non-lesional skin[12-16].

In previous studies, it has been shown that AE is strongly associated with mutations in the filaggrin gene (*FLG*)[17-19], but the role of FLG mutations for the barrier dysfunction is yet inconclusive[20-25]. Other factors, such as aberrations in the SC lipids, may play a role in the decreased skin barrier in AE[12,26,27]. In healthy SC, lipids form two lamellar phases with repeat distances of approximately 6 and 13 nm. These are referred to as the short periodicity phase (SPP) and long periodicity phase (LPP), respectively[28,29]. A schematic presentation of the lipid organization is provided in Figure 3. Within the lipid lamellae, the lipids have a dense (orthorhombic) lateral organization, although a subpopulation of the lipids can be less densely packed in a hexagonal organization[30-32].

CERs play a crucial role in the lipid organization[33], and they have a characteristic molecular architecture. Several studies have reported significant changes in CER subclasses in non-lesional SC of AE patients: reduced CER [NP], increased CER [AS], and reduced long chain CERs [EOH] and [EOS][12,23,34-36]. Some of these changes could be correlated with changes in skin barrier function. However, no information was reported on the effect of chain length distribution of CERs on the skin barrier until recently: Ishikawa *et al*. showed that lesional skin has a significantly increased level of short-chain CERs (with a total chain length of 34 carbon atoms) in one specific CER subclass, which correlates with the impaired skin barrier function[37]. These results suggest that CER chain length may be an important factor in skin barrier dysfunction of AE patients. These findings were the starting point of the present study, in which we performed a detailed analysis on CER composition, focusing in particular on the CER chain length distribution in non-lesional SC of AE patients in relation to lipid organization and skin barrier dysfunction. We studied SC of non-lesional skin, as we aimed to monitor the changes in lipid properties in the absence of inflammation. We have identified several CER subclasses that exhibit an increased level of extremely short C34 chains in AE, and we demonstrate that the overall level of C34 is increased in AE. The changes in CER chain length distribution correlated with changes in lipid organization, skin barrier function, disease severity, and levels

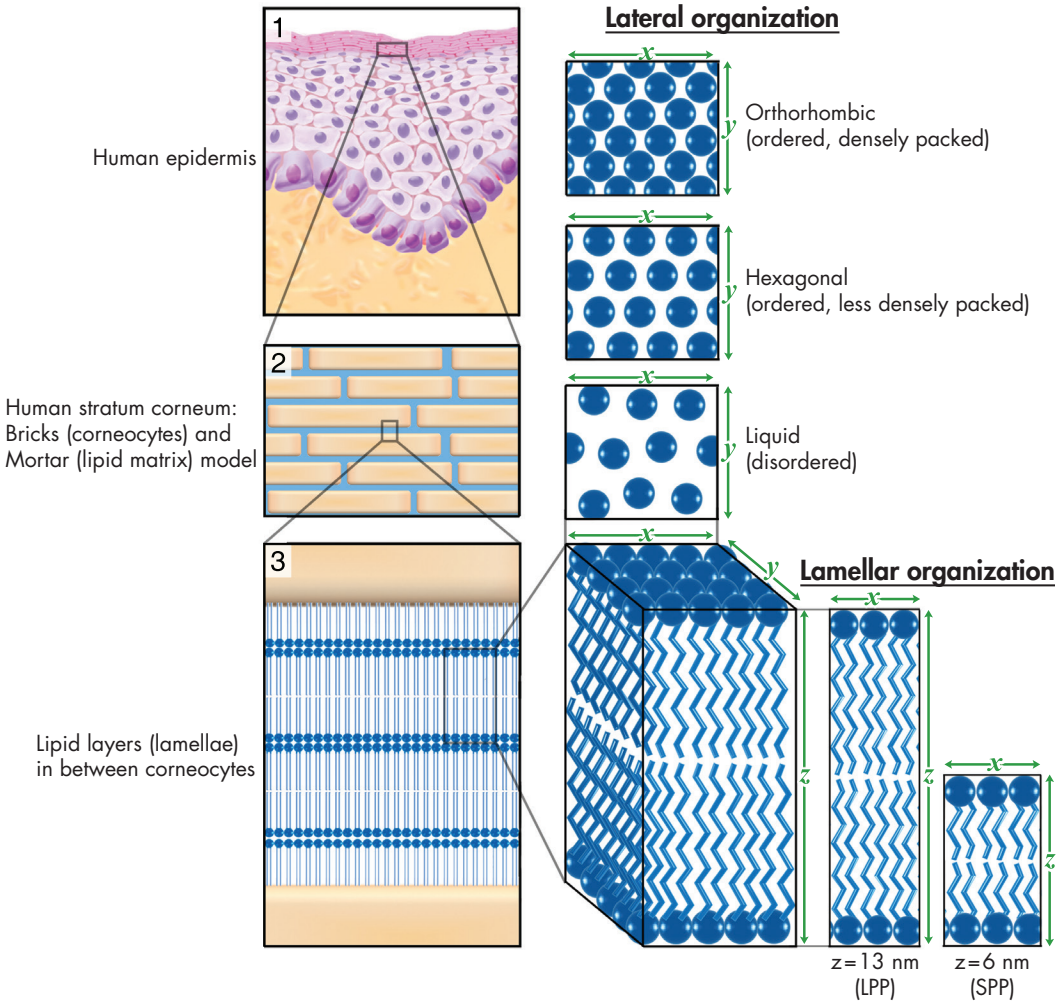

Figure 3: *Lamellar and lateral organization in human stratum corneum.* ***a****) The outermost layer of the epidermis, the stratum corneum (SC), consists of dead cells (corneocytes) embedded in a lipid matrix, also referred to as the brick (corneocytes) and mortar (lipids) structure* ***b****). The intercellular lipids are arranged in layers (lamellae)* ***c****), with two coexisting lamellar phases. These lamellar phases have a repeat distance of 6 nm (referred to as the short periodicity phase (SPP)) or 13 nm (referred to as the long periodicity phase (LPP)). The lateral organization is the plane perpendicular to the direction of the lamellar organization. There are three possible arrangements of the lipids: a very dense, ordered, orthorhombic organization; a less dense, ordered, hexagonal organization; or a disordered, liquid organization.*

of natural moisturizing factor (NMF, composed of filaggrin-derived amino acids, their metabolites, specific sugars, and salts). Changes in CER chain length distribution did not correlate with *FLG* genotype. These results demonstrate for the first time that CER chain length is an important factor in skin barrier dysfunction in non-lesional skin of AE.

Material and Methods

Study population and general study setup

The study was conducted in accordance with the Declaration of Helsinki Principles, and was approved by the Ethical Committee of the Leiden University Medical Center. All subjects gave written informed consent. 15 Caucasian subjects without (history of) dermatological disorders (25.0 ± 5.2 years; 5 males) and 28 Caucasian AE patients (25.6 ± 5.6 years; 11 males) were included. The group of AE patients consists of 14 patients with and 14 patients without the presence of common *FLG* genotype mutations (see *FLG* mutation analysis below). Subjects did not apply any dermatological products to their forearms for at least one week prior to the study. The study itself was performed in a temperature and humidity controlled room, and subjects were acclimatized for 45 min prior to the measurements. Per subject, all measurements were performed on a single day on one of the ventral forearms, which was observed by a dermatologist at the start of the study to carefully depict an area of non-lesional skin, which was marked accordingly. At this area, NMF levels were determined with Raman spectroscopy, followed by subsequent tape stripping, TEWL, and Fourier transform infrared spectroscopy (FTIR) measurements, as described below. At the end of the study day, buccal mucosa cells were collected with a cotton swab, and SCORing Atopic Dermatitis (SCORAD) was performed by a dermatologist to determine the severity of the disease. Finally, a 4 mm biopsy was harvested close to the area where all measurements were performed.

FLG mutation analysis

The influence of *FLG* mutations on lipid properties was studied. We screened all subjects on the four most prevalent mutations found in European Caucasians (*2282del4, R501X, S3247X* and *R2447X*), covering around 93% of all *FLG* mutations known to date[38]. Buccal mucosa cells were collected by rubbing the inside of the cheeks with a cotton swab on a plastic stick after rinsing the mouth with water. Mutations were determined by genotyping after DNA extraction[39].

Skin barrier function assessment by TEWL

A Tewameter 210 (Courage+Khazaka, Köln, Germany) was used to measure TEWL on the marked area on the ventral forearm of the subject. The forearm was placed in an open chamber, and TEWL values were recorded for 2 minutes, after which an average reading during the last 10 seconds of the measurement was calculated. This procedure was performed before tape stripping (baseline TEWL) and after every two tape strips to have an indication of the amount of removed SC.

SCORAD

SCORAD was performed by the dermatologist to determine the severity of the disease[40].

Determination of NMF levels in SC

Confocal Raman microspectroscopy (3510 Skin Composition Analyzer, River Diagnostics, Rotterdam, The Netherlands) was used to measure NMF in the SC of the ventral forearm. The principles and experimental details of this method and the procedure have been described elsewhere[41,42]. Depth profiles of Raman spectra were measured at 2 μm intervals from the skin surface to 20 μm below the skin surface. In each subject, 15 profiles were measured at different spots within the marked area on the ventral forearm. Raman spectra were recorded between 400 and 1800 cm^{-1} with a 785 nm laser. Laser power on the skin was 25 mW. NMF levels relative to keratin were determined from the Raman spectra measured between 4 and 8 μm by means of classical least-squares fitting. Relative NMF to keratin levels were calculated from the recorded Raman spectra by using SkinTools 2.0 (River Diagnostics, Rotterdam, The Netherlands).

Tape stripping procedure

To harvest SC lipids, the following tape stripping procedure was performed on both control subjects and non-lesional regions of AE patients: multiple poly(phenylene sulfide) tape strips (Nichiban, Tokyo, Japan) were successively applied at the same area (4.5 cm^2) on the ventral forearm. All tapes were pressed to the targeted skin with a pressure of 450 g/cm^2 using a D-Squame pressure instrument (Cuderm Corp., Dallas, TX). Tweezers were used to remove the tape in a fluent stroke, using alternating directions for each successive tape strip. The Squamescan 850A (Heiland Electronic, Wetzlar, Germany) was used to determine the amount of SC removed to obtain a good indication of the depth of each tape strip taken[43,44]. Calibration was performed by a bicinchoninic acid (BCA) assay using bovine serum albumin (BSA). The predicted total amount of protein in the SC was calculated by plotting 1/TEWL against the cumulative amount of protein removed. The intercept with the x-axis is indicative for the total amount of protein in the SC according to Kalia *et al.*[43]. Tapes 6 to 9 were selected for lipid composition analysis, as these tapes do not show surface contamination (observed when analyzing tape strips from the surface of the SC). All tapes were punched to a circular area of 2 cm^2, put individually into glass vials containing 1 mL chloroform/methanol/water (1:2:½) and stored at -20°C under argon atmosphere prior to lipid extraction.

Lipid extraction and ceramide analysis by LC/MS

Lipid extraction was performed on 4 tape strips (numbers 6 to 9) of each subject. Before lipids were extracted from tape strips by liquid-liquid extraction, 2 deuterated internal ceramide standards (CER [NS] C24 and, CER [EOS] C30 linoleate) were added to compare CER levels between control group and non-lesional skin of AE patients. Then, a slightly enhanced extraction procedure of the commonly used Bligh and Dyer method was performed on all 4 selected tape strips individually: 3 different ratios of solvent mixtures chloroform/methanol/water (1:2:½; 1:1:0; 2:1:0) were used sequentially to extract all lipids. A detailed procedure is described elsewhere[45,46]. Afterwards, lipid extracts from all 4 individual tapes were pooled, dried under N_2 gas and reconstituted in 100 µl chloroform/methanol/heptane (2½:2½:95) to obtain a total lipid concentration around 1.0 mg/mL. Samples were stored at -20°C until use. The analysis was performed by LC/MS using a recently developed LC/MS method described in detail elsewhere[4]. Briefly, 10 µl of each lipid sample was automatically injected and separated onto an analytical normal phase column (PVA-bonded column; 100 × 2.1 mm i.d., 5 µm particle size, YMC (Kyoto, Japan)) by a gradient solvent system from heptane to heptane/IPA/ethanol at a flow rate of 0.8 mL/min using an Alliance 2695 HPLC system (Waters Milford, MA). The HPLC was coupled to a mass spectrometer (TSQ Quantum, Thermo Finnigan, San Jose, CA) in atmospheric pressure chemical ionization (APCI), positive scan mode with a scan range set at 360-1200 amu. The temperature of the source heater and heated capillary were set to 450°C and 250°C, respectively, and the discharge current was set to 5 µA. The ceramide analysis was performed using Xcalibur software version 2.0, and its nomenclature used throughout this article is according to Motta *et al.*[47] in which ceramide subclasses are classified by letter abbreviations according to their two individual chains: the sphingoid base (either dihydrosphingosine (dS), sphingosine (S), 6-hydroxy sphingosine (H) or phyto-sphingosine (P)), chemically linked to the fatty acid chain (either an α-hydroxy fatty acid (A), an esterified ω-hydroxy fatty acid (EO) or a non-hydroxy fatty acid (N)). This results in 12 different CER subclasses, namely [AdS], [AS], [AH], [AP], [EOdS], [EOS], [EOH], [EOP], [NDS], [NS], [NH], and [NP]. The CER nomenclature and its molecular structure are explained in Figure 1.

Lateral organization and conformational ordering of the lipids

To obtain information on the lateral organization and conformational ordering of the lipids, FTIR spectra were recorded in the same skin region also used for lipid analysis. FTIR spectra of the SC were collected after each 2 tape strips using a Varian 670-IR spectrometer (Varian Inc., Santa Clara, CA) equipped with a broad band mercury-

cadmium-telluride (MCT) detector and an external sample compartment containing a GladiATR (Pike, Madison, WI) attenuated total reflection (ATR) accessory with a single reflection diamond. The spectral resolution was 2 cm^{-1}. The instrument was continuously purged with dry N_2. Each spectrum was an average of 150 scans. For data treatment the instrument software Resolutions Pro 4.1 (Varian Inc.) was used. We calculated positions of the CH_2 symmetric stretching vibration and second derivatives of the scissoring bandwidth as described previously[48,49]. Shortly, the second derivative was calculated and it was baseline-corrected between the endpoints of the scissoring region (~1460-1480 cm^{-1}). We calculated the bandwidth at 50% of the peak height (full width half maximum, FWHM) and determined CH_2 symmetric stretching vibration positions of spectra recorded between the removal of 2 to 10 tape strips.

Biopsy and small angle X-ray diffraction measurements

After tape stripping, 4 mm biopsies were taken from the ventral forearm close to the region of the tape stripping. SC was isolated by trypsin digestion as described earlier[50]. This procedure does not affect the lipid organization in SC[51]. The SC sheets were measured by small angle X-ray diffraction (SAXD) performed at the European Synchrotron Radiation Facility (ESRF, Grenoble, France) using station BM26B. Prior to the measurements, SC was hydrated over a 27% NaBr solution during 24h. To obtain high quality diffraction patterns SC was carefully oriented parallel to the primary X-ray beam. SAXD patterns were detected with a Frelon 2000 charge-coupled device (CCD) detector at room temperature for a period of 10 minutes using a microfocus beam, similarly as described elsewhere[52]. Samples were checked for evidence of radiation damage, and exposure time to X-rays was kept to a minimum. From the scattering angle, the scattering vector (q) was calculated by $q = 4\pi \sin\theta/\lambda$, in which λ is the wavelength of the X-rays at the sample position and θ the scattering angle.

Statistical analysis

Statistical analysis was performed using SPSS Statistics. Non-parametric Mann-Whitney tests were performed when comparing 2 groups and stated significant when $P<0.05$. When the effect of *FLG* was taken into account and trends were observed, Kruskall-Wallis tests, and eventually, additional Mann-Whitney tests were performed. Bivariate analysis was performed to analyze which parameters showed a significant correlation, and their respective Spearman's ρ correlation coefficients were calculated. Univariate general linear model analysis was performed to correlate the biologically and clinically relevant parameters to 2 independent lipid parameters, as well as to the predicted and the observed average chain length.

Results

Description of study population

Fourteen out of 28 AE patients were carriers of at least one of the four most common *FLG* mutations (details in Supplementary Table I). Patient and control subject characteristics are provided in Supplementary Table II. Two control subjects were heterozygous for *FLG* mutations. Severity of the disease was scored by an experienced dermatologist using SCORAD (Figure 4a). AE patients showed an elevated TEWL in non-lesional skin compared with control subjects (12.2 ± 6.5 g/m²/h and 6.5 ± 1.7 g/m²/h, respectively; $P<0.0005$, Figure 4b) and lower NMF levels compared with control subjects (0.66 ± 0.39 and 1.05 ± 0.20, respectively; $P<0.01$, Figure 4c).

Reduced CER chain length correlates with a decreased barrier function

From the LC/MS data, lipid profiles were constructed and examples are shown in Supplementary Figure 1. From manual integration of these lipid profiles, the relative abundance of all CER subclasses could be calculated (Supplementary Figure 2). Statistical differences between control subjects and AE patients were observed in 7 subclasses: CERs [EOP], [EOH], [NS], [NP], [NH], [AS] and [AH] ($P<0.05$). No difference was observed between carriers and non-carriers of *FLG* mutations. The total CER level in the control group and in non-lesional skin of AE patients was not significantly different 37.0 ± 3.6 and 38.5.4 ± 2.4 ng/µg protein, respectively ($P>0.1$).

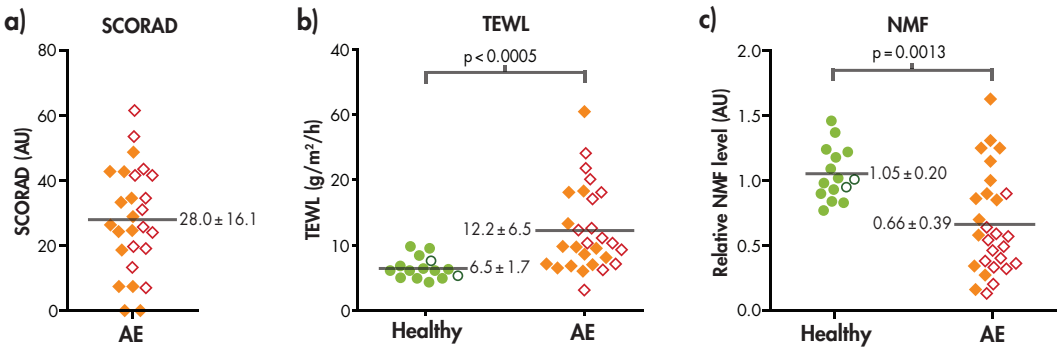

Figure 4: *SCORAD, TEWL and NMF levels in control subjects and AE patients. Dot plots showing individual control subjects (○ and ●) and AE patients (◇ and ◆) of the measured parameters (**a**) SCORAD, (**b**) TEWL and (**c**) NMF levels. Open and filled data points indicate carriers and non-carriers of NMF mutations, respectively. Means are indicated by gray horizontal lines and their corresponding values (±SD). Significant differences were observed between control subjects and AE patients for both TEWL and NMF. FLG mutations were associated with reduced NMF levels in AE patients ($P<0.005$) but not with SCORAD and TEWL.*

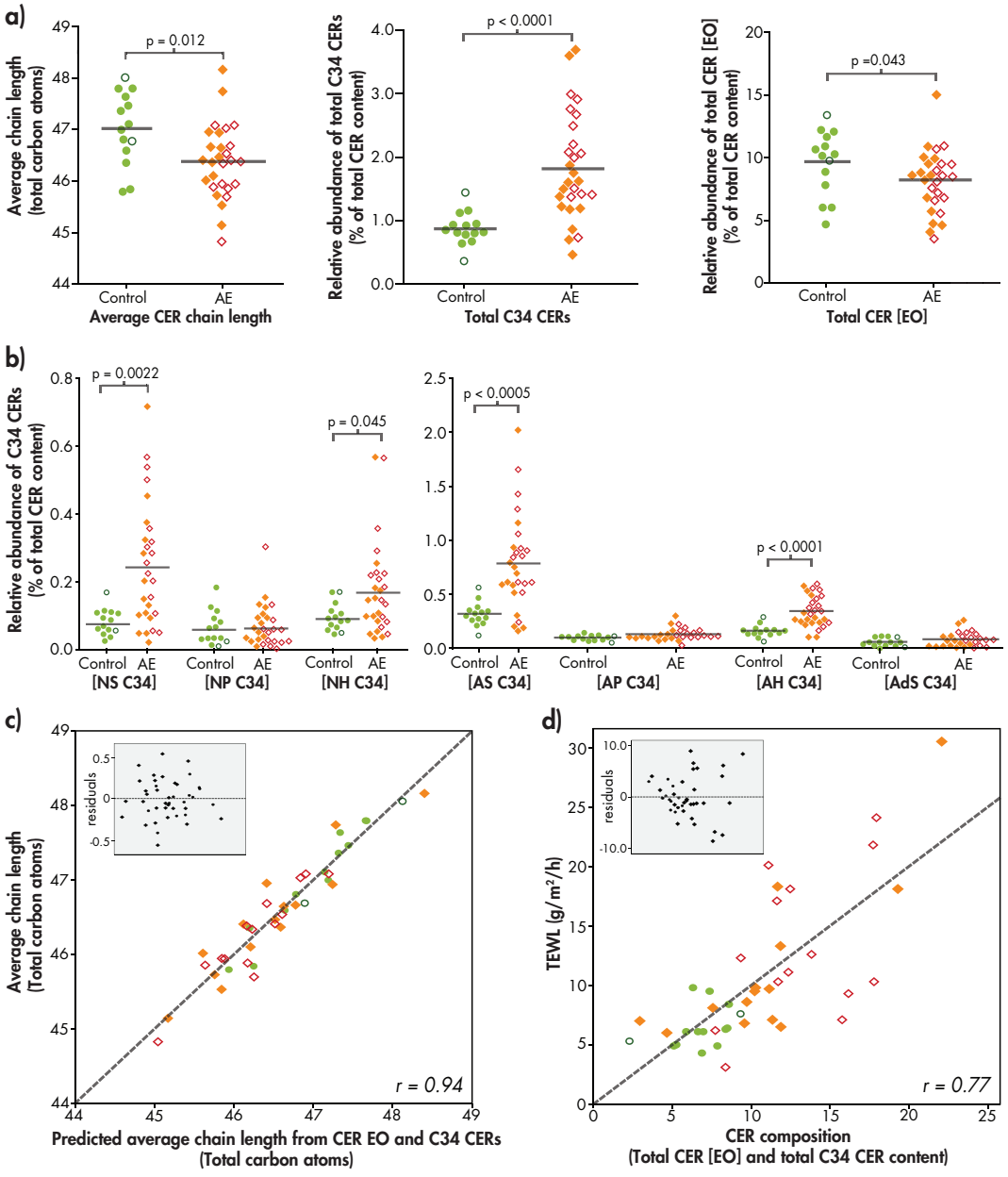

Figure 5: *CER composition in control subjects and AE patients.* ***a****) Dot plot showing the average chain length of all CERs in total; the relative abundance of total C34 CERs; and the relative abundance of total [EO] CERs.* ***b****) Dot plots indicating the relative abundance of C34 CER species for each subclass.* ***c****) Scatter plot of univariate analysis of the predicted average chain length (by the abundance of C34 CERs and [EO] CERS) versus the observed average chain length. Gray dotted lines represents the optimal fit (r=0.94).* ***d****) Scatter plot of univariate analysis of C34 CER and CER [EO] versus the TEWL. Insets show the residuals of the respective plots. Gray dotted lines represents the optimal fit (r=0.77). Control subjects are indicated by ○ and ●. AE patients with are indicated by ◇ and ◆. Open and filled data points indicate carriers and non-carriers of FLG mutations, respectively.*

The average CER chain length was significantly decreased by 0.64 ± 0.23 total carbon atoms in AE patients (mean±SEM; P=0.012, Figure 5a). No difference was observed between carriers and non-carriers of *FLG* mutations (P>0.1). Figure 5a shows that in non-lesional skin of AE patients, extremely short C34 CERs were increased within several CER subclasses. This was primarily observed in CER subclasses [AS], [AH], [NS] and [NH] (Figure 5b, P<0.05). The increase in total C34 CERs in AE (P<0.0001) contributes to a reduction in overall chain length. In addition, the very long chain CERs belonging to the [EO] subclass are significantly reduced, which is primarily caused by significantly decreased levels of CER [EOH] and [EOP] (P=0.019 and P=0.040, respectively, Figure 5a and Supplementary Figure 2b). Univariate analysis shows that an increased level of C34 CERs and decreased level of CERs [EO] largely contribute to a reduction in average CER chain length, as can be observed from Figure 5c. The influence of *FLG* mutations on any of the CER chain length parameters was not significant (P>0.1; detailed overview in Supplementary Tables III-V).

The observed changes in CER chain length were compared with changes in barrier function as assessed by TEWL. The results in Figure 5d show a strong correlation between TEWL and the levels of C34 CERs and CER [EO]: univariate analysis of TEWL versus the total C34 CERs and total CER [EO] levels shows a correlation coefficient of 0.77 (P<0.0001). Correlations between the relative abundances of the various CER subclasses with TEWL are shown in Table I. CER [EOH] and CER [AS] are the two subclasses which are most significantly associated with TEWL. This again indicates the importance of the chain length for the skin barrier in AE: the exceptional long CER [EOH] is decreased, whereas CER [AS] (the CER subclass with the highest abundance of exceptionally short C34 CERs) is increased. The changes in CER composition are irrespective of *FLG* mutation status (P=0.58).

CER subclass	TEWL
CER [EOdS]	-0.245
CER [EOS]	-0.177
CER [EOP]	-0.434**
CER [EOH]	**-0.617*** **
CER [NdS]	-0.226
CER [NS]	0.407**
CER [NP]	-0.483**
CER [NH]	-0.420**
CER [AdS]	0.214
CER [AS]	**0.650*** **
CER [AP]	0.255
CER [AH]	0.195
Total CER [EO]	-0.441**
Total C34 CERs	**0.738*** **
Average CER chain length	**0.528*** **

Table I: *Correlation coefficients of the various CER subclasses versus TEWL. The table contains all 12 CER subclasses as well as the CERs that strongly influence the chain length (i.e. total CER [EO] and total C34 CERs).*

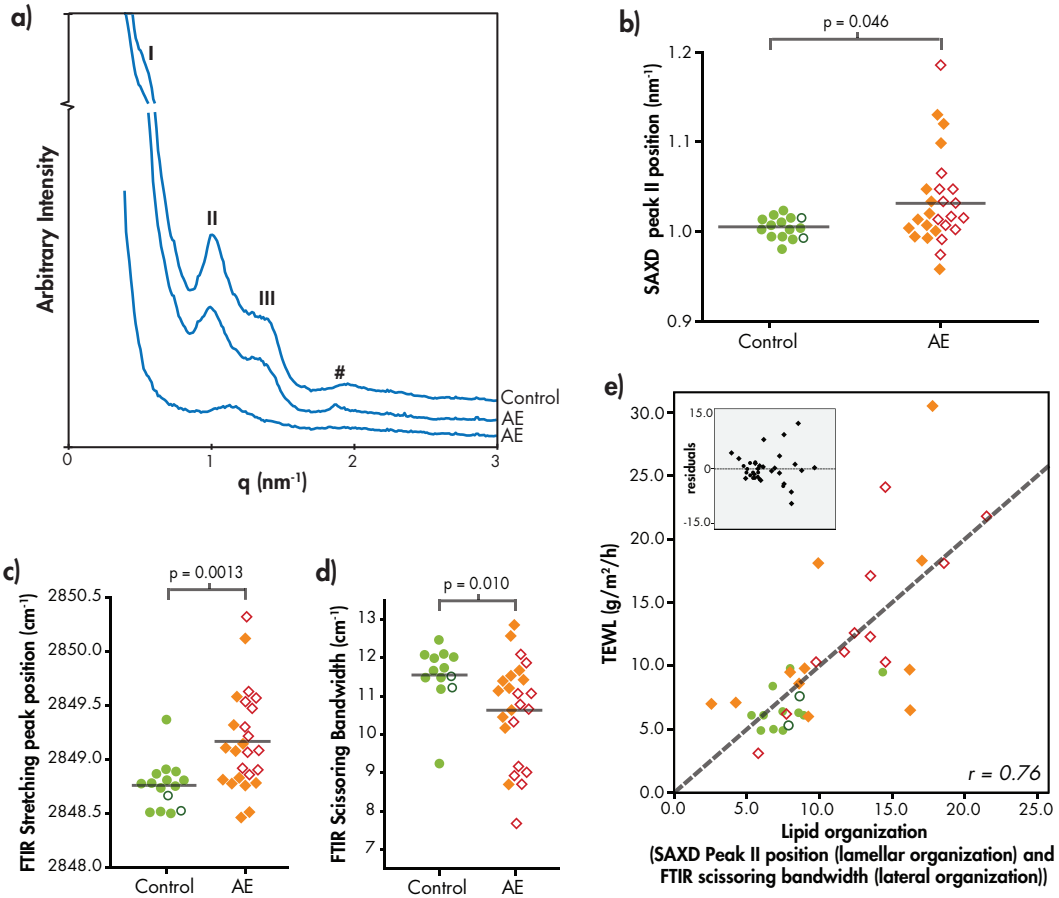

Figure 6: *Lipid organization in control subjects and AE patients.* ***a****) The upper SAXD curve of a control subject shows the 1st (I), 2nd (II) and 3rd (III) order peak positions of the LPP. # indicates phase separated cholesterol. The middle diffraction curve is from an AE patient and resembles the pattern of SC of the control subject. The bottom curve of an AE patient shows only the presence of peak II.* ***b****) Position of peak II in SAXD curves.* ***c****) Position of the stretching vibrations in the FTIR spectrum.* ***d****) Scissoring bandwidth in the FTIR spectrum.* ***e****) Correlation between lipid organization and TEWL. Scatter plot of univariate analysis of SAXD peak II position + bandwidth of scissoring vibrations versus the TEWL. The inset shows the residuals of this plot. The gray dotted line represents the optimal fit (r=0.76). Control subjects are indicated by ○ and ●. AE patients with are indicated by ◇ and ◆. Open and filled data points indicate carriers and non-carriers of FLG mutations, respectively.*

Altered lamellar and lateral lipid organization correlates with a decreased barrier function

SAXD gives information about the lamellar organization of intercellular lipids in SC[28] (explanation in Supplementary Figure 3). The lipids form two lamellar phases, the SPP and LPP. Figure 6a shows three examples of SAXD curves from SC. The upper curve is a typical example of a control subject. The central curve is typical for AE. The bottom curve

is representative for a subgroup of AE patients with an aberrant SAXD profile. The upper two curves show lipid-based features as two weak diffraction peaks (labeled I and III) and a strong peak (labeled II). The LPP contributes to all three peaks, whereas the SPP contributes only to peak II (Supplementary Figure 3). In the bottom curve, both peaks I and III are absent, and peak II is shifted to higher *q*-values. Peaks I and III were not present in 5 out of 28 patients. As peak I and peak III are attributed to the LPP, this indicates that there is a drastic reduction in the presence of the LPP in those patients.

Figure 6b shows the position of the strong peak (II) in the SAXD curves from control subjects (left) and AE patients (right). The peak position shows a larger variance within the group of AE patients compared with the group of control subjects. The average position of the strong peak is located at significantly higher *q*-values for AE patients compared with control subjects (1.03 nm^{-1} and 1.00 nm^{-1}, respectively, P=0.046). The position of peak II showed no difference between AE patients with and patients without *FLG* mutations (P=0.76).

FTIR was used to obtain information on the lateral lipid organization. Two types of vibrations were monitored, the CH_2 symmetric stretching vibrations and the CH_2 scissoring vibrations (Supplementary Figure 4). A low (~2848 cm^{-1}) wavenumber of the CH_2 symmetric stretching vibrations indicates the presence of a highly ordered lipid organization (either hexagonal or orthorhombic), whereas a high (2853 cm^{-1}) wavenumber indicates a liquid disordered phase[53]. The mean value of the position of the CH_2 symmetric stretching vibrations of AE patients shows a small but significant shift to higher values compared with control subjects (2849.2 cm^{-1} versus 2848.8 cm^{-1}, respectively, P=0.0013, Figure 6c). In addition, the variance in the group of AE patients is larger than in control subjects. To distinguish between an orthorhombic (dense) or hexagonal (less dense) lateral organization, the bandwidth of the CH_2 scissoring vibrations was monitored. A narrow bandwidth (typically 8 cm^{-1}) indicates the presence of only a hexagonal lipid organization, whereas a large bandwidth of typically 11 cm^{-1} is indicative for the presence of mainly an orthorhombic organization[49]. The average bandwidth of the scissoring vibrations was significantly lower in AE patients compared with control subjects (10.6 cm^{-1} versus 11.6 cm^{-1}, respectively, P=0.010, Figure 6d), demonstrating a reduction of lipids in an orthorhombic organization and thus a less dense lipid organization. No significant influence of *FLG* mutations on the lipid organization in AE patients was found (P>0.05, Figures 6b-d).

Univariate analysis was performed between TEWL and two independent lipid organization parameters: a lamellar organization component (SAXD peak II position) and a lateral organization component (*FTIR* scissoring bandwidth). The correlation coefficient

Lipid organization / CER composition parameters	Correlation coefficients (r)
SAXD peak II position vs total C34 CER content	0.432**
SAXD peak II position vs total CER [EO] content	-0.393**
SAXD peak II position vs average CER chain length	-0.370*
FTIR scissoring bandwidth vs total C34 CER content	-0.669***
FTIR scissoring bandwidth vs total CER [EO] content	0.267
FTIR scissoring bandwidth vs average CER chain length	0.386*
FTIR stretching vs total C34 CER content	0.607***
FTIR stretching vs total CER [EO] content	-0.399*
FTIR stretching vs average CER chain length	-0.471**

Table II: *Correlation coefficients of lipid composition and lipid organization parameters.*

Correlated parameters	Correlation coefficients (r)
TEWL vs SCORAD	0.560**
TEWL vs SAXD peak II position	0.450**
TEWL vs FTIR scissoring bandwidth	-0.735**
TEWL vs FTIR stretching	0.645**
TEWL vs total C34 CER content	0.738**
TEWL vs total CER [EO] content	-0.441**
TEWL vs average CER chain length	-0.528**
TEWL vs NMF	-0.643**
SCORAD vs SAXD peak II position	0.164
SCORAD vs FTIR scissoring bandwidth	-0.474*
SCORAD vs FTIR stretching	0.534**
SCORAD vs total C34 CER content	-0.470*
SCORAD vs total CER [EO] content	-0.238
SCORAD vs average CER chain length	-0.265
SCORAD vs NMF	-0.362*
NMF vs SAXD peak II position	-0.501**
NMF vs FTIR scissoring bandwidth	0.697**
NMF vs FTIR stretching	-0.778**
NMF vs total C34 CER content	-0.611**
NMF vs total CER [EO] content	0.416**
NMF vs average CER chain length	0.456**

Table III: *Correlations between the various parameters.*

was r=0.76 (P<0.0001, Figure 6e), which demonstrates that skin barrier function as measured by TEWL is significantly influenced by lipid organization.

Altered CER composition correlates with aberrant lipid organization.

As the CER composition and lipid organization both show a relationship with a reduced skin barrier (TEWL), the relation between the lipid parameters is summarized in Table II. The levels of C34 CERs and CER [EO] associate with both the lamellar organization (SAXD) and lateral lipid organization (FTIR scissoring bandwidth and stretching vibrations position). A powerful correlation of 0.71 was observed when both the lamellar and lateral organization components (SAXD and CH_2 scissoring) were plotted versus the two components of the CER composition ([EO] CERs and C34 CERs). Supplementary Figure 5 illustrates this correlation.

Altered CER composition and aberrant lipid organization correlate with NMF levels and SCORAD

A detailed overview of correlation coefficients between different parameters is presented in Table III. NMF levels correlate ($r>0.4$, $P<0.01$) with both lamellar and lateral lipid organization as well as with chain length of the CERs. SCORAD (disease severity) was associated with CER composition (i.e. total C34 CERs and total CER [EO] content) and lipid organization (i.e. SAXD peak II position and *FTIR* scissoring bandwidth), with correlation coefficients of 0.56 ($P<0.01$) and 0.58 ($P<0.01$), respectively.

***FLG* mutations correlate with NMF levels, but not with SCORAD and TEWL levels.**

NMF levels were significantly lower in FLG carriers than in non-carriers (0.45 ± 0.19 and 0.87 ± 0.43, respectively, $P<0.005$). Both SCORAD and TEWL values were independent of *FLG* genotype ($P=0.34$ and $P=0.23$), respectively.

Discussion

We performed an integral analysis of CER composition, focusing on the chain length distribution of each of the CER subclasses in relation to lipid organization and their correlation with skin barrier function (TEWL), disease severity (SCORAD), *FLG* mutations and NMF levels. This study provides detailed information about the role of lipids in the impaired skin barrier function of non-lesional AE skin.

The results show a reduced average CER chain length in non-lesional skin of AE patients. This reduction in chain length can be attributed to an increase in extremely short C34 CERs as well as a reduction in very long CER [EO] subclasses. The increment in C34 CERs has recently been reported by Ishikawa *et al*. for a single subclass (CER [NS]) in lesional skin of AE patients[37]. Here we show in non-lesional skin a largely increased level of C34 CERs in four CER subclasses: CER [NS], [NH], [AS] and [AH]. In addition, the results show changed levels in some of the CER subclasses consistent with previous reports: a decrease in CER [NP] level and an increase in CER [AS] level[12,34-37,54,55]. We did not observe a change in CER/protein levels between AE patients and controls. Interestingly, the reduction in CER chain length found in the present study had a much stronger impact on the skin barrier function than did the changes in CER subclass levels: the TEWL increases proportionally with decreasing chain length. These findings are in excellent agreement with earlier *in vitro* studies showing that a reduction in chain length of CERs has a stronger impact on the lipid organization and permeability than a change in the ratio between CER subclasses keeping the chain length approximately equal56-58, unpublished results M. Oguri, G.S. Gooris, J.A. Bouwstra). Di Nardo *et al*. observed a reduction in CER/CHOL ratio in non-

lesional skin of AE patients, whereas other studies do not report a decrease in CER content in non-lesional AE skin[20,35-37,54]. Groen *et al*.[58] observed that when increasing the CER or FFA level while keeping the level of the other two main lipid classes equal, did not affect the permeability *in vitro*. Therefore these studies suggest that the CER composition and chain length rather than the ratio between lipid classes does play a major role in the increased TEWL in non-lesional skin in patients with AE. The increment in C34 CERs and decrement in CER [EO] suggest that elongation of the acyl chains is reduced. As the elongase family plays an important role in the elongation of fatty acids in the viable epidermis, we hypothesize that the higher abundance of C34 CERs may be due to a misbalance in the activity of some of the members of the elongase family[59,60].

Several publications report on the lipid organization in AE patients: Pilgram *et al*. reported changes in the lateral packing when comparing three AE patients with three controls[32]. In a very recent study, we reported the first results on a very limited number of subjects focusing on the lamellar phases and ceramide subclasses without examining the CER chain lengths[61]. In addition, several studies focused on the (delayed or incomplete) lamellar body extrusion process in AE[62-64], possibly caused by a reduced peroxisome proliferator-activated receptor activation[65]. In the present study we were particularly interested in the influence of CER chain length on the lipid organization in AE patients.

With respect to the lamellar lipid organization, we observed a shift in the peak II position of SAXD curves of SC in AE patients. This observation indicates a reduced value of the repeat distances of the lamellar phases and/or a reduced formation of the LPP[28]. The correlation between SAXD peak II position with CER [EO] and C34 CER levels indicates that changes in these CER levels affect the lamellar organization. When focusing on the lateral organization, AE patients show a less dense lipid packing compared with controls that correlates strongly with a higher level of C34 CERs. This finding shows that CER chain length is also an important determinant of the lateral lipid organization in SC. The observed changes in lamellar and lateral organization correlate with the increased TEWL levels and thus with an abnormal skin barrier function in patients with AE. The findings in this study strongly support the hypothesis that in AE patients a reduction in CER chain length leads to a change in lipid organization, which in turn leads to an impaired barrier function. In addition, the present study shows that this impaired barrier function is correlated with the disease severity as determined by SCORAD, which is supported by literature[66,67]. This may indicate that as a result of inflammation, lipid synthesis is influenced (even at non-lesional sites), and subsequently the barrier function is decreased.

As *FLG* mutations are known to be predisposing factors for AE[17], an interesting question is whether lipid changes are associated with the presence of *FLG* mutations. We

screened our subjects for four of the most prevalent *FLG* mutations accounting for 93% of the European *FLG* mutation spectrum[38]. In our study cohort, there is no evidence that *FLG* mutations have an effect on CER composition and lipid organization. In contrast, in a recent study in ichtyosis vulgaris patients[68], changes in the lamellar organization were observed between the patients and controls. In that investigation, however, the majority of the patients were homozygote or compound heterozygote with respect to *FLG* mutations, and no inflammation was observed in these patients.

In previous studies, as well as in the current study, AE patients with *FLG* mutations showed significantly reduced NMF levels[22,69]. Remarkably, in this study changes in lipids correlated with NMF levels but not with the presence or absence of *FLG* mutations. This suggests that between *FLG* gene (genotype) and NMF (phenotype), other (translational and environmental) factors may also influence NMF levels. These factors may include *FLG* copy numbers (repeat alleles on the *FLG* gene)[70] and interleukin levels, which can downregulate filaggrin expression[71]. Changes in NMF levels are suggested to lead to a change in pH, and together with altered interleukin levels and protease activity this may affect enzymes involved in CER biosynthesis[5,68,72-74] and therefore change the CER composition and lipid organization. Thus, despite the fact that we did not find a correlation between the lipids and *FLG* mutation status, filaggrin might play an indirect role in the decreased barrier function of AE patients, although the underlying mechanism remains unclear. Besides, other barrier proteins may be involved. This will be subject of future studies by our group. In conclusion, in this study we have shown that the CER chain length is altered in AE patients by elevated C34 CERs levels and reduced CER [EO] levels. These changes correlate with an altered lipid organization and a decreased barrier function in AE patients. In addition, a significant correlation was observed between disease severity and change in lipid composition and organization. Our results suggest a novel therapeutic entry to repair skin barrier defects in AE patients, aimed at normalizing CER chain length distribution. Such a treatment could improve the SC lipid organization and restore the skin barrier function of AE patients.

Acknowledgements

This research is supported by the European Cooperation in Science and Technology (COST) and the Dutch Technology Foundation STW, which is part of the Netherlands Organisation for Scientific Research (NWO), and which is partly funded by the Ministry of Economic Affairs. The authors thank Cosmoferm for provision of the synthetic CERs and the Netherlands Organization for Scientific Research (NWO) for provision of beam time.

References

1 Proksch E, Folster-Holst R, Jensen JM. Skin barrier function, epidermal proliferation and differentiation in eczema. *J Dermatol Sci* 2006; 43: 159-69.

2 Elias PM, Menon GK. Structural and lipid biochemical correlates of the epidermal permeability barrier. *Adv Lipid Res* 1991; 24: 1-26.

3 Masukawa Y, Narita H, Sato H *et al.* Comprehensive quantification of ceramide species in human stratum corneum. *J Lipid Res* 2009; 50: 1708-19.

4 van Smeden J, Hoppel L, van der Heijden R *et al.* LC/MS analysis of stratum corneum lipids: ceramide profiling and discovery. *J Lipid Res* 2011; 52: 1211-21.

5 Cork MJ, Robinson DA, Vasilopoulos Y *et al.* New perspectives on epidermal barrier dysfunction in atopic dermatitis: gene-environment interactions. *J Allergy Clin Immunol* 2006; 118: 3-21; quiz 2-3.

6 Leung DY, Bieber T. Atopic dermatitis. *Lancet* 2003; 361: 151-60.

7 Alanne S, Nermes M, Soderlund R *et al.* Quality of life in infants with atopic dermatitis and healthy infants: a follow-up from birth to 24 months. *Acta Paediatr* 2011; 100: e65-70.

8 Mozaffari H, Pourpak Z, Pourseyed S *et al.* Quality of life in atopic dermatitis patients. *J Microbiol Immunol Infect* 2007; 40: 260-4.

9 Slattery MJ, Essex MJ, Paletz EM *et al.* Depression, anxiety, and dermatologic quality of life in adolescents with atopic dermatitis. *J Allergy Clin Immunol* 2011; 128: 668-71 e3.

10 van Valburg RW, Willemsen MG, Dirven-Meijer PC *et al.* Quality of life measurement and its relationship to disease severity in children with atopic dermatitis in general practice. *Acta Derm Venereol* 2011; 91: 147-51.

11 Williams H, Flohr C. How epidemiology has challenged 3 prevailing concepts about atopic dermatitis. *Journal of Allergy and Clinical Immunology* 2006; 118: 209-13.

12 Di Nardo A, Wertz P, Giannetti A *et al.* Ceramide and cholesterol composition of the skin of patients with atopic dermatitis. *Acta Derm Venereol* 1998; 78: 27-30.

13 Yoshiike T, Aikawa Y, Sindhvananda J *et al.* Skin barrier defect in atopic dermatitis: increased permeability of the stratum corneum using dimethyl sulfoxide and theophylline. *J Dermatol Sci* 1993; 5: 92-6.

14 Werner Y, Lindberg M. Transepidermal water loss in dry and clinically normal skin in patients with atopic dermatitis. *Acta Derm Venereol* 1985; 65: 102-5.

15 Seidenari S, Giusti G. Objective assessment of the skin of children affected by atopic dermatitis: A study of pH, capacitance and TEWL in eczematous and clinically uninvolved skin. *Acta Dermato-Venereologica* 1995; 75: 429-33.

16 Elias PM, Schmuth M. Abnormal skin barrier in the etiopathogenesis of atopic dermatitis. *Current Opinion in Allergy and Clinical Immunology* 2009; 9: 437-46.

17 Palmer CN, Irvine AD, Terron-Kwiatkowski A *et al.* Common loss-of-function variants of the epidermal barrier protein filaggrin are a major predisposing factor for atopic dermatitis. *Nat Genet* 2006; 38: 441-6.

18 Hudson TJ. Skin barrier function and allergic risk. *Nature Genetics* 2006; 38: 399-400.

19 Seguchi T, ChangYi C, Kusuda S *et al.* Decreased expression of filaggrin in atopic skin. *Archives of Dermatological Research* 1996; 288: 442-6.

20 Angelova-Fischer I, Mannheimer AC, Hinder A *et al.* Distinct barrier integrity phenotypes in filaggrin-related atopic eczema following sequential tape stripping and lipid profiling. *Exp Dermatol* 2011; 20: 351-6.

21 Jakasa I, Koster ES, Calkoen F *et al.* Skin barrier function in healthy subjects and patients with atopic dermatitis in relation to filaggrin loss-of-function mutations. *J Invest Dermatol* 2011; 131: 540-2.

22 O'Regan GM, Kemperman PM, Sandilands A *et al.* Raman profiles of the stratum corneum define 3 filaggrin genotype-determined atopic dermatitis endophenotypes. *J Allergy Clin Immunol* 2010; 126: 574-80 e1.

23 Jungersted JM, Scheer H, Mempel M *et al.* Stratum corneum lipids, skin barrier function and filaggrin mutations in patients with atopic eczema. *Allergy* 2010; 65: 911-8.

24 Flohr C, England K, Radulovic S *et al.* Filaggrin loss-of-function mutations are associated with early-onset eczema, eczema severity and transepidermal water loss at 3 months of age. *Br J Dermatol* 2010; 163: 1333-6.

25 Landstad BJ, Ekholm J, Broman L *et al.* Working environmental conditions as experienced by women working despite pain. *Work* 2000; 15: 141-52.

26 Elias PM. Stratum corneum defensive functions: An integrated view. *Journal of Investigative Dermatology* 2005; 125: 183-200.

27 Elias PM, Steinhoff M. "Outside-to-Inside" (and now back to "Outside") pathogenic mechanisms in atopic dermatitis. *Journal of Investigative Dermatology* 2008; 128: 1067-70.

28 Bouwstra JA, Gooris GS, van der Spek JA *et al.* Structural investigations of human stratum corneum by small-angle X-ray scattering. *J Invest Dermatol* 1991; 97: 1005-12.

29 Madison KC, Swartzendruber DC, Wertz PW *et al.* Presence of intact intercellular lipid lamellae in the upper layers of the stratum corneum. *J Invest Dermatol* 1987; 88: 714-8.

30 Ongpipattanakul B, Francoeur ML, Potts RO. Polymorphism in stratum corneum lipids. *Biochim Biophys Acta* 1994; 1190: 115-22.

31 Bommannan D, Potts RO, Guy RH. Examination of stratum corneum barrier function in vivo by infrared spectroscopy. *J Invest Dermatol* 1990; 95: 403-8.

32 Pilgram GS, Vissers DC, van der Meulen H *et al.* Aberrant lipid organization in stratum corneum of patients with atopic dermatitis and lamellar ichthyosis. *J Invest Dermatol* 2001; 117: 710-7.

33 Bouwstra JA, Ponec M. The skin barrier in healthy and diseased state. *Biochim Biophys Acta* 2006; 1758: 2080-95.

34 Bleck O, Abeck D, Ring J *et al.* Two ceramide subfractions detectable in Cer(AS) position by HPTLC in skin surface lipids of non-lesional skin of atopic eczema. *J Invest Dermatol* 1999; 113: 894-900.

35 Farwanah H, Raith K, Neubert RH *et al.* Ceramide profiles

of the uninvolved skin in atopic dermatitis and psoriasis are comparable to those of healthy skin. *Arch Dermatol Res* 2005; 296: 514-21.
36 Imokawa G, Abe A, Jin K *et al.* Decreased level of ceramides in stratum corneum of atopic dermatitis: an etiologic factor in atopic dry skin? *J Invest Dermatol* 1991; 96: 523-6.
37 Ishikawa J, Narita H, Kondo N *et al.* Changes in the ceramide profile of atopic dermatitis patients. *J Invest Dermatol* 2010; 130: 2511-4.
38 Chen H, Common JE, Haines RL *et al.* Wide spectrum of filaggrin-null mutations in atopic dermatitis highlights differences between Singaporean Chinese and European populations. *Br J Dermatol* 2011; 165: 106-14.
39 Sandilands A, Terron-Kwiatkowski A, Hull PR *et al.* Comprehensive analysis of the gene encoding filaggrin uncovers prevalent and rare mutations in ichthyosis vulgaris and atopic eczema. *Nat Genet* 2007; 39: 650-4.
40 Stalder JF, Taieb A. Severity scoring of atopic dermatitis: the SCORAD index. Consensus Report of the European Task Force on Atopic Dermatitis. *Dermatology* 1993; 186: 23-31.
41 Caspers PJ, Lucassen GW, Carter EA *et al.* In vivo confocal Raman microspectroscopy of the skin: noninvasive determination of molecular concentration profiles. *J Invest Dermatol* 2001; 116: 434-42.
42 Caspers PJ, Lucassen GW, Puppels GJ. Combined in vivo confocal Raman spectroscopy and confocal microscopy of human skin. *Biophys J* 2003; 85: 572-80.
43 Kalia YN, Alberti I, Naik A *et al.* Assessment of topical bioavailability in vivo: the importance of stratum corneum thickness. *Skin Pharmacol Appl Skin Physiol* 2001; 14 Suppl 1: 82-6.
44 Voegeli R, Heiland J, Doppler S *et al.* Efficient and simple quantification of stratum corneum proteins on tape strippings by infrared densitometry. *Skin Res Technol* 2007; 13: 242-51.
45 Bligh EG, Dyer WJ. A rapid method of total lipid extraction and purification. *Can J Biochem Physiol* 1959; 37: 911-7.
46 Thakoersing VS, Ponec M, Bouwstra JA. Generation of human skin equivalents under submerged conditions-mimicking the in utero environment. *Tissue Eng Part A* 2010; 16: 1433-41.
47 Motta S, Monti M, Sesana S *et al.* Ceramide composition of the psoriatic scale. *Biochim Biophys Acta* 1993; 1182: 147-51.
48 Boncheva M, Damien F, Normand V. Molecular organization of the lipid matrix in intact Stratum corneum using ATR-FTIR spectroscopy. *Biochim Biophys Acta* 2008; 1778: 1344-55.
49 Damien F, Boncheva M. The extent of orthorhombic lipid phases in the stratum corneum determines the barrier efficiency of human skin in vivo. *J Invest Dermatol* 2010; 130: 611-4.
50 Tanojo H, BosvanGeest A, Bouwstra JA *et al.* In vitro human skin barrier perturbation by oleic acid: Thermal analysis and freeze fracture electron microscopy studies. *Thermochimica Acta* 1997; 293: 77-85.
51 Schreiner V, Gooris GS, Pfeiffer S *et al.* Barrier characteristics of different human skin types investigated with X-ray diffraction, lipid analysis, and electron microscopy imaging. *J Invest Dermatol* 2000; 114: 654-60.
52 Bras W, Dolbnya IP, Detollenaere D *et al.* Recent experiments on a combined small-angle/wide-angle X-ray scattering beam line at the ESRF. *Journal of Applied Crystallography* 2003; 36: 791-4.
53 Moore DJ, Rerek ME, Mendelsohn R. FTIR spectroscopy studies of the conformational order and phase behavior of ceramides. *Journal of Physical Chemistry B* 1997; 101: 8933-40.
54 Yamamoto A, Serizawa S, Ito M *et al.* Stratum corneum lipid abnormalities in atopic dermatitis. *Arch Dermatol Res* 1991; 283: 219-23.
55 Matsumoto M, Umemoto N, Sugiura H *et al.* Difference in ceramide composition between "dry" and "normal" skin in patients with atopic dermatitis. *Acta Derm Venereol* 1999; 79: 246-7.
56 de Jager M, Groenink W, Bielsa i Guivernau R *et al.* A novel in vitro percutaneous penetration model: evaluation of barrier properties with p-aminobenzoic acid and two of its derivatives. *Pharm Res* 2006; 23: 951-60.
57 de Sousa Neto D, Gooris G, Bouwstra J. Effect of the omega-acylceramides on the lipid organization of stratum corneum model membranes evaluated by X-ray diffraction and FTIR studies (Part I). *Chem Phys Lipids* 2011; 164: 184-95.
58 Groen D, Poole DS, Gooris GS *et al.* Is an orthorhombic lateral packing and a proper lamellar organization important for the skin barrier function? *Biochim Biophys Acta* 2011; 1808: 1529-37.
59 Ohno Y, Suto S, Yamanaka M *et al.* ELOVL1 production of C24 acyl-CoAs is linked to C24 sphingolipid synthesis. *Proc Natl Acad Sci U S A* 2010; 107: 18439-44.
60 Park YH, Jang WH, Seo JA *et al.* Decrease of ceramides with very long-chain fatty acids and downregulation of elongases in a murine atopic dermatitis model. *J Invest Dermatol* 2012; 132: 476-9.
61 Janssens M, van Smeden J, Gooris GS *et al.* Lamellar lipid organization and ceramide composition in the stratum corneum of patients with atopic eczema. *J Invest Dermatol* 2011; 131: 2136-8.
62 Fartasch M, Bassukas ID, Diepgen TL. Disturbed extruding mechanism of lamellar bodies in dry non-eczematous skin of atopics. *Br J Dermatol* 1992; 127: 221-7.
63 Marsella R, Samuelson D, Doerr K. Transmission electron microscopy studies in an experimental model of canine atopic dermatitis. *Vet Dermatol* 2010; 21: 81-8.
64 Scharschmidt TC, Man MQ, Hatano Y *et al.* Filaggrin deficiency confers a paracellular barrier abnormality that reduces inflammatory thresholds to irritants and haptens. *J Allergy Clin Immunol* 2009; 124: 496-506, e1-6.
65 Man MQ, Barish GD, Schmuth M *et al.* Deficiency of PPARbeta/delta in the epidermis results in defective cutaneous permeability barrier homeostasis and increased inflammation. *J Invest Dermatol* 2008; 128: 370-7.
66 Chamlin SL, Kao J, Frieden IJ *et al.* Ceramide-dominant barrier repair lipids alleviate childhood atopic dermatitis: changes in barrier function provide a sensitive indicator of disease activity. *J Am Acad Dermatol* 2002; 47: 198-208.
67 Nemoto-Hasebe I, Akiyama M, Nomura T *et al.* Clinical

severity correlates with impaired barrier in filaggrin-related eczema. *J Invest Dermatol* 2009; 129: 682-9.

68 Gruber R, Elias PM, Crumrine D *et al.* Filaggrin genotype in ichthyosis vulgaris predicts abnormalities in epidermal structure and function. *Am J Pathol* 2011; 178: 2252-63.

69 Kezic S, Kemperman PM, Koster ES *et al.* Loss-of-function mutations in the filaggrin gene lead to reduced level of natural moisturizing factor in the stratum corneum. *J Invest Dermatol* 2008; 128: 2117-9.

70 Irvine AD, McLean WHI, Leung DYM. MECHANISMS OF DISEASE Filaggrin Mutations Associated with Skin and Allergic Diseases. *New England Journal of Medicine* 2011; 365: 1315-27.

71 Howell MD, Kim BE, Gao P *et al.* Cytokine modulation of atopic dermatitis filaggrin skin expression. *J Allergy Clin Immunol* 2007; 120: 150-5.

72 Hachem JP, Man MQ, Crumrine D *et al.* Sustained serine proteases activity by prolonged increase in pH leads to degradation of lipid processing enzymes and profound alterations of barrier function and stratum corneum integrity. *J Invest Dermatol* 2005; 125: 510-20.

73 Nakagawa N, Sakai S, Matsumoto M *et al.* Relationship between NMF (lactate and potassium) content and the physical properties of the stratum corneum in healthy subjects. *J Invest Dermatol* 2004; 122: 755-63.

74 Schmid-Wendtner MH, Korting HC. The pH of the skin surface and its impact on the barrier function. *Skin Pharmacol Physiol* 2006; 19: 296-302.

Supplementary Material

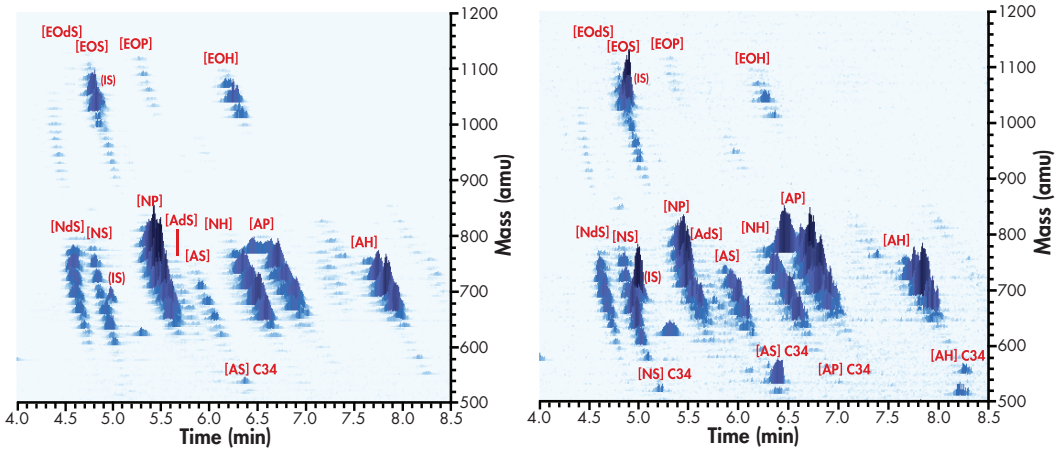

Supplementary Figure 1: *Representative 3D multi-mass chromatograms of SC ceramides of a healthy subject (left) and an AE patient (right). All subclasses are indicated by their abbreviation. IS indicates one of the deuterated internal standards (CER classes [EOS] and [NS]) which were added to every sample to enable semi-quantitative analysis.*

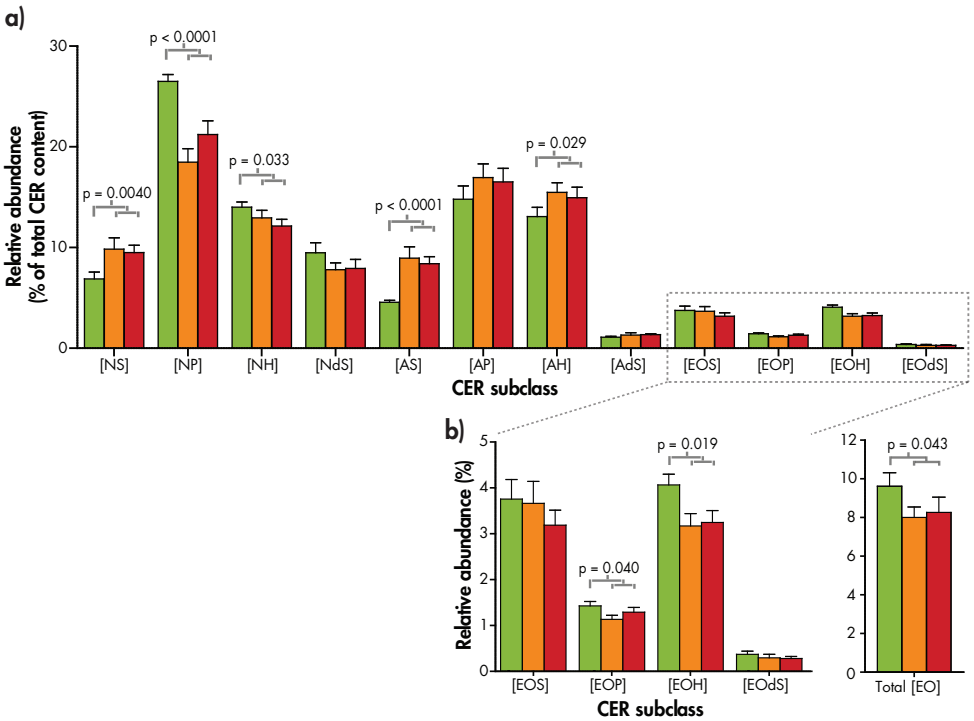

Supplementary Figure 2: *Bar plot showing the relative abundances of all CER subclasses (**a**) and only the very long [EO] CER subclasses (**b**) (Mean ± SEM). Green bars correspond to the control group, while orange and red bars correspond to AE patients who do not and do carry FLG mutations, respectively.*

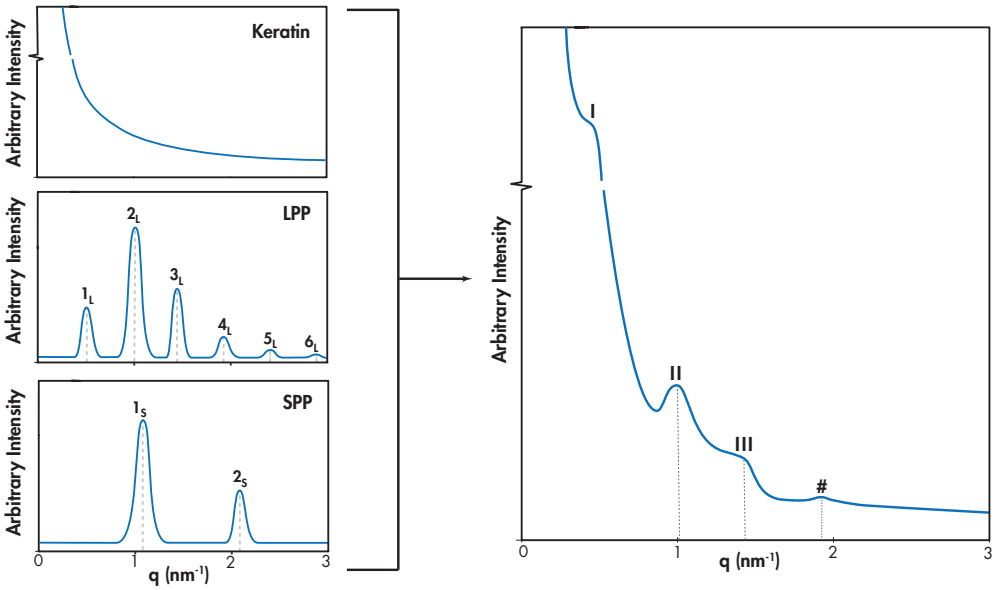

Supplementary Figure 3: *Lamellar organization in human stratum corneum. The right graph shows a typical SAXD profile of human SC. The scattering intensity (I) is plotted as a function of q, which is defined by* $q = 2\pi \sin \theta/\lambda$*, in which* λ *is the wavelength of the X-rays and* θ *the angle of the scattered x-rays. The X-ray diffraction graph of human stratum corneum is characterized by a high intensity at low q values due to keratin in the corneocytes and a series of peaks. The peaks indicated by I (weak peak), II (strong peak) and III (weak peak) are attributed to the LPP. Peak II is also attributed to the SPP. The peak indicated by # is due to cholesterol. A schematic drawing of the X-ray curves of the keratin, LPP and SPP is also shown on the left. The 1st, 2nd, 3rd, 4th, 5th and 6th order of the LPP (indicated by 1L-6L) and 1st and 2nd order of the SPP (indicated by 1S and 2S) . From the positions of the peaks (q) the repeat distance of the LPP and SPP can be calculated using the equation* $d = n \cdot 2\pi/q_n$ *(n = order of diffraction peak). When comparing the positions of the LPP and SPP to that in the diffraction pattern of the SC, peak I and III are only attributed to the LPP, while II is attributed to the LPP (2L) and SPP (1S). Higher order reflections cannot be detected due to the low intensities of these peaks.*

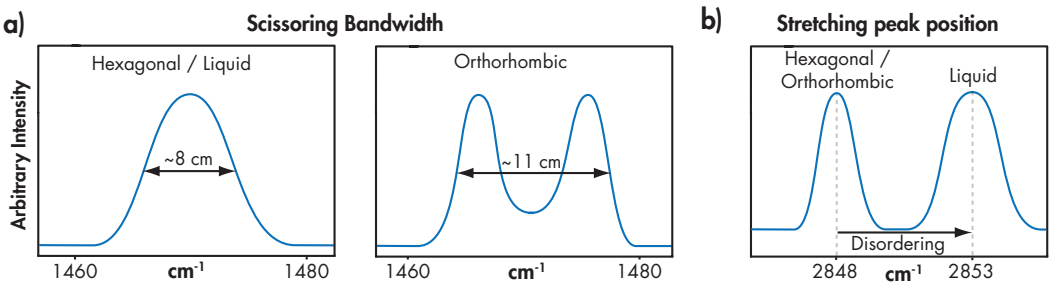

Supplementary Figure 4: *The lateral organization can be measured by Fourier transform infrared spectroscopy (FTIR) by focusing on the* CH_2 *scissoring vibrations (1460-1480 cm*$^{-1}$*) and the* CH_2 *symmetric stretching vibrations (2848-2053 cm*$^{-1}$*).* ***a****) An orthorhombic organization results in a splitting of the scissoring vibrations, while a hexagonal packing results in a single vibration. Therefore, an increased bandwidth of the scissoring vibrations is indicative for an increased fraction of lipids forming orthorhombic lipid domains. In addition, the* CH_2 *symmetric stretching vibration provides information about the conformational ordering of the lipids* ***b****); a lower frequency (~2848 cm*$^{-1}$*) indicates a fully extended chains (high degree of conformational ordering) of the lipids, whereas a high wavenumber (2853 cm*$^{-1}$*) is indicative for a liquid organization (low degree of conformational ordering).*

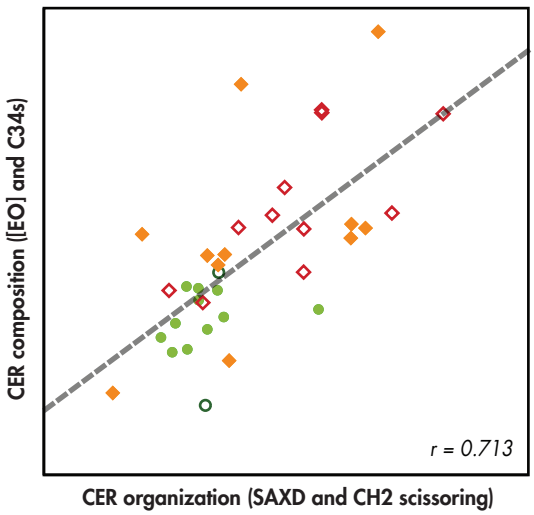

Supplementary Figure 5: *Scatter plot of univariate analysis of the predicted correlation between the CER organization (lamellar organization (SAXD) and lateral organization (CH_2 scissoring) versus the CER organization (the abundance of [EO] CERS and C34 CERs). Gray dotted line represents the optimal fit (r=0.713). Control subjects are indicated by ●/○. Non-lesional skin and lesional skin of AE patients are indicated by ◆/◇ and ■/□.Open and filled data points indicate carriers and non-carriers of FLG mutations, respectively.*

Supplementary Table I. *Mutations in the cohort of AE patients.*

Loss-of-function mutation	2282del4	R501X	R2447X	S3247X
Heterozygous:10	4	4	1	1
Homozygous: 3	2	1	-	-
Compound heterozygous: 1	1	1	-	-

Supplementary Table II. *Characteristics of the subjects*

Parameter	Control (n=15)	AE (n=28)
Age (years)	25.0 ± 5.2	25.6 ± 5.6
Female gender	10	17
Total SCORAD	-	28.0 ± 16.1
TEWL ($g/m^2/h$)	6.5 ± 1.7	12.2 ± 6.5
NMF (AU)	1.05 ± 0.2	0.66 ± 0.39
FLG mutation	2	14

Supplementary Table III. *Statistical data of the relative abundance of the 12 CER subclasses in control subjects versus AE patients and AE patients that carry and do not carry FLG mutations.*

CER subclass	Control (%, mean ± SD)	AE (%, mean ± SD)	Statistical significance (*P*-value)	*FLG* mutation in patients (%, mean ± SD)	No *FLG* mutation in patients (%, mean ± SD)	Statistical significance (*P*-value)
[EOS]	3.76 ± 0.59	3.43 ± 1.52	0.191	3.66 ± 1.79	3.19 ± 1.22	0.550
[EOP]	1.43 ± 0.36	1.21 ± 0.36	0.040	1.13 ± 0.33	1.29 ± 0.38	0.270
[EOH]	4.06 ± 0.87	3.21 ± 0.97	0.019	3.17 ± 1.01	3.25 ± 0.97	0.783
[EOdS]	0.37 ± 0.26	0.29 ± 0.23	0.286	0.30 ± 0.28	0.28 ± 0.17	0.713
[NS]	6.88 ± 2.57	9.67 ± 3.44	0.003	9.84 ± 4.20	9.51 ± 2.64	0.646
[NP]	26.5 ± 2.57	19.85 ± 5.16	<0.001	18.49 ± 4.99	21.21 ± 5.14	0.183
[NH]	14.01 ± 1.94	12.54 ± 2.63	0.033	12.94 ± 2.83	12.14 ± 2.45	0.462
[NdS]	9.48 ± 3.75	7.86 ± 2.92	0.063	7.80 ± 2.59	7.92 ± 3.32	0.783
[AS]	4.57 ± 0.68	8.67 ± 3.48	<0.001	8.95 ± 4.24	8.39 ± 2.65	0.963
[AP]	14.79 ± 4.96	16.73 ± 4.94	0.308	16.95 ± 5.05	16.52 ± 5.02	0.890
[AH]	13.07 ± 3.46	15.21 ± 3.66	0.028	15.47 ± 3.59	14.96 ± 3.84	0.462
[AdS]	1.09 ± 0.32	1.32 ± 0.66	0.272	1.30 ± 0.88	1.35 ± 0.36	0.141

Supplementary Table IV. *Data of the relative abundance of all C34 CERs between control versus AE and AE patients that carry and do not carry FLG mutations. CA is the total number of carbon atoms.*

CER	Control (%, mean ± SD)	AE (%, mean ± SD)	Statistical significance (*P*-value)	*FLG* mutation in patients (%, mean ± SD)	No *FLG* mutation in patients (%, mean ± SD)	Statistical significance (*P*-value)
[AS] C34	0.32 ± 0.11	0.78 ± 0.44	<0.001	0.68 ± 0.48	0.89 ± 0.38	0.089
[AP] C34	0.10 ± 0.02	0.13 ± 0.06	0.058	0.13 ± 0.07	0.13 ± 0.05	0.232
[AH] C34	0.16 ± 0.06	0.34 ± 0.14	<0.001	0.30 ± 0.14	0.39 ± 0.13	0.089
[AdS] C34	0.06 ± 0.04	0.08 ± 0.07	0.337	0.07 ± 0.08	0.09 ± 0.05	0.251
[NS] C34	0.08 ± 0.04	0.25 ± 0.18	0.002	0.22 ± 0.20	0.28 ± 0.17	0.198
[NP] C34	0.06 ± 0.05	0.07 ± 0.06	0.936	0.07 ± 0.04	0.06 ± 0.08	0.141
[NH] C34	0.10 ± 0.04	0.17 ± 0.14	0.045	0.14 ± 0.14	0.20 ± 0.14	0.118

Supplementary Table V. *Statistical overview of the relative abundance regarding CER [EO] and CERs C34 for control subjects and AE patients. The effect of FLG mutations in patients is shown as well.*

Parameter	Control (mean ± SD)	AE (mean ± SD)	Statistical significance (*P*-value)	*FLG* mutation in patients (mean ± SD)	No *FLG* mutation in patients (mean ± SD)	Statistical significance (*P*-value)
CER [EO] (%)	9.62 ± 2.62	8.13 ± 2.47	0.079*	8.26 ± 2.94	8.00 ± 2.00	0.788*
CERs C34 (%)	0.87 ± 0.26	1.83 ± 0.83	0.00017*	1.62 ± 0.95	2.04 ± 0.68	0.185*
Mean chain length (CA)	47.0 ± 0.72	46.4 ± 0.72	0.012**	46.7 ± 0.78	46.4 ± 0.74	0.277**